First Measurements of the Index of Refraction of Gases for Lithium Atomic Waves

M. Jacquey, M. Büchner, G. Trénec, and J. Vigué*

Laboratoire Collisions Agrégats Réactivité-IRSAMC, Université Paul Sabatier and CNRS UMR 5589, 118, route de Narbonne, 31062 Toulouse Cedex, France

(Received 21 November 2006; published 15 June 2007)

We report the first measurements of the index of refraction of gases for lithium waves. Using an atom interferometer, we have measured the real and imaginary parts of the index of refraction n for argon, krypton, and xenon as a function of the gas density for several velocities of the lithium beam. The linear dependence of $(n-1)$ with the gas density is well verified. The total collision cross section deduced from the imaginary part of $(n-1)$ is in very good agreement with traditional measurements of this quantity. Finally, the real and imaginary parts of $(n-1)$ and their ratio ρ exhibit glory oscillations, in good agreement with calculations.

DOI: 10.1103/PhysRevLett.98.240405 PACS numbers: 03.75.Be, 03.75.Dg, 34.20.−b, 39.20.+q

The concept of the index of refraction for waves transmitted through matter was extended from light waves to neutron waves around 1940, as reviewed by Lax [1]. The extension to atom waves was done in 1995 with the first measurements of the index of refraction of gases for sodium waves [2] and the subsequent observation of glory oscillations on the index variations with sodium velocity [3–6]. We report here the first measurements of the index of refraction of gases for lithium waves.

Several papers [7–16] have dealt with the theory of the index of refraction n. The index of refraction is proportional to the forward scattering amplitude, which can be calculated if the interaction potential between an atom of the wave and an atom of the target gas is known. The imaginary part of the forward scattering amplitude is related to the total cross section but its real part can be measured only by atom interferometry. This amplitude exhibits resonances, for a collision energy comparable to the potential well depth, and glory oscillations, for larger energy. These glory oscillations are due to the existence of an undeflected classical trajectory resulting from the compensation of attractive and repulsive forces [17].

A measurement of the index of refraction thus provides a new access to atom-atom interaction potentials. Many other experiments are sensitive to the atom-atom interaction potentials: in the particular case of alkali-rare gas pairs, measurements of total and differential cross sections, line broadening experiments, and spectroscopy of van der Waals molecules have been much used. Each technique is more sensitive to a different part of the potential curve and one would expect that very accurate potentials are available, but, as shown by the calculations done in Refs. [5,15,16], the index of refraction deduced from various potentials differ substantially, thus proving the need for more accurate potentials.

Our experiment is similar to the experiments of [2,3,5]. We have measured separately the real and imaginary parts of $(n-1)$ with a good accuracy and tested their linear dependence with the gas density. The total collision cross section deduced from our measurement of the imaginary part $\mathrm{Im}(n-1)$ is in very good agreement with previous measurements [18,19]. Our measurements of the real and imaginary parts of $(n-1)$ and of their ratio ρ are in good agreement with the calculations done by Champenois [16], using potential curves fitted in Refs. [18,19].

The principle of the experiment is to introduce some gas on one of the atomic beams inside an atom interferometer, as represented in Fig. 1. Noting $\psi_{u/l}$, the waves propagating on the upper or lower paths inside the interferometer, the interference signal I is given by

$$I = |\psi_l + \psi_u \exp(i\varphi)|^2. \quad (1)$$

The phase $\varphi = k_G(2x_2 - x_1 - x_3)$, which depends on the grating positions x_i (k_G is the grating wave vector), is used to observe interference fringes. We can rewrite Eq. (1) as

$$I = I_B + I_0[1 + \mathcal{V}\cos(\varphi)]. \quad (2)$$

I_0 is the mean intensity, $\mathcal{V}$ the fringe visibility, and we have added the detector background I_B. When the atomic

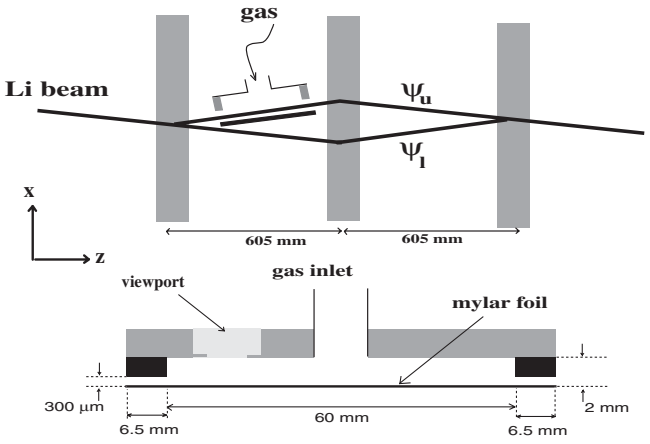

FIG. 1. Upper part: Schematic drawing of a top view of the interferometer, with the gas cell inserted just ahead of the second laser standing wave. Lower part: Top view of the gas cell. The viewport is used to align the septum by optical techniques. The slit widths are exaggerated to be visible.

wave propagates in a gas of density n_{gas}, its wave vector $\mathbf{k}$ becomes $n\mathbf{k}$, where n is the index of refraction. For a gas cell of length L in the upper path, the wave ψ_u is replaced by the transmitted wave $\psi_{u,t}$ given by

$$\psi_{u,t}/\psi_u = \exp[i(n-1)kL] = t(n_{\mathrm{gas}})\exp[i\varphi(n_{\mathrm{gas}})], \quad (3)$$

with $t(n_{\mathrm{gas}}) = \exp[-\mathrm{Im}(n-1)kL]$ and $\varphi(n_{\mathrm{gas}}) = \mathrm{Re}(n-1)kL$. The signal given by Eq. (2) is modified, with a phase shift $\varphi(n_{\mathrm{gas}})$. The mean intensity $I_0(n_{\mathrm{gas}})$ and the fringe visibility $\mathcal{V}(n_{\mathrm{gas}})$ are both changed and $t(n_{\mathrm{gas}})$ is related to these quantities by

$$t(n_{\mathrm{gas}}) = I_0(n_{\mathrm{gas}})\mathcal{V}(n_{\mathrm{gas}})/[I_0(0)\mathcal{V}(0)]. \quad (4)$$

Our Mach-Zehnder atom interferometer uses laser diffraction in the Bragg regime [20], with a laser wavelength close to the lithium first resonance line at 671 nm. To optimize the signal for the ^{7}Li isotope with first order diffraction, we have used a frequency detuning equal to 4 GHz, a total laser power equal to 275 mW, and a beam waist radius $w_0 = 6.2$ mm. The lithium beam mean velocity u is varied by seeding lithium in a rare gas mixture and the velocity distribution thus achieved has a full width at half maximum close to 25%.

For a mean atom velocity $u = 1075$ m/s, the maximum distance between the atomic beam centers, close to 100 μm, is sufficient to insert a septum between these beams. The septum, a 6 μm thick mylar foil, separates the gas cell from the interferometer vacuum chamber. This cell is connected to the interferometer chamber by 300 μm wide slits, as shown in Fig. 1, in order to reduce the gas flow. The cell is connected by a 16 mm diameter ultrahigh vacuum gas line to a leak valve used to introduce the gas. Another valve connects the gas line to the interferometer vacuum chamber so that the cell pressure can be reduced to its base value in about 3 s. We use high purity gases from Air Liquide (total impurity content below 50 ppm) and a cell pressure in the 10^{-3}–10^{-4} mbar range. The pressure is measured by a membrane gauge (Leybold CERAVAC CTR91), with an accuracy near 1%. When the cell is evacuated, the measured pressure, $p_{\mathrm{meas}} = (1 \pm 1) \times 10^{-6}$ mbar, is negligible. Because of the gas flow through the connection pipe, the cell pressure p_{cell} is slightly less than the measured value p_{meas} as the gauge is at about 50 cm from the cell. Molecular flow theory predicts that the pressure in the cell p_{cell} is homogeneous within 1% and that $p_{\mathrm{cell}}/p_{\mathrm{meas}} = C_{\mathrm{pipe}}/(C_{\mathrm{pipe}} + C_{\mathrm{slits}})$. The conductances of the pipe, C_{pipe}, and of the slits, C_{slits}, have been calculated and we get $p_{\mathrm{cell}}/p_{\mathrm{meas}} = 0.90 \pm 0.01$. We then use the ideal gas law at $T = 298$ K to deduce the gas density n_{gas} in the cell.

We record interference fringes by displacing the third standing wave mirror with a linear voltage ramp applied on a piezoelectric stage. In order to correct the interferometer phase drift, each experiment is made of three sweeps, the first and third ones ($j = 1$ and 3) with an empty cell and the second one ($j = 2$) with a pressure p_{cell}. The counting time is 0.3 s per data point, with 300 points per sweep. After the third sweep, we flag the lithium beam to measure the detector background I_B. We assume that the phase φ can be written $\varphi = a_j + b_j n + c_j n^2$, where the quadratic term describes the nonlinearity of the piezo stage (n being the channel number). The best fit of each recording, using Eq. (2), provides the initial phase a_j, the mean intensity I_{0j}, and the fringe visibility $\mathcal{V}_j$. We thus get the effect of the gas, namely, the phase shift $\varphi(n_{\mathrm{gas}}) = a_2 - (a_1 + a_3)/2$, and the attenuation $t(n_{\mathrm{gas}})$ given by Eq. (4) [the $I_0(0)\mathcal{V}(0)$ value is taken as the mean of the $j = 1$ and $j = 3$ values].

For a given lithium mean velocity u, we measure the phase shift and the amplitude attenuation for various gas pressures and we plot $\varphi(n_{\mathrm{gas}})$ and $-\ln[t(n_{\mathrm{gas}})]$ as a function of pressure (see Fig. 2). These two quantities are expected to vary linearly with the gas density [2–4] and the high signal to noise ratio of our experiments allows us to confirm these theoretical expectations. To deduce $(n-1)$ from this plot, we need the kL value. k is calculated from the lithium beam mean velocity u measured by Bragg diffraction. The effective cell length L is calculated by weighting each element dz by the local gas density. In the molecular regime, the density in the slits varies linearly with z and vanishes near the slit exit [21]. The effective length L is then the sum of the inner part length and of the mean of the slit lengths, $L = 66.5 \pm 1.0$ mm. Our final results are the real and imaginary parts of $(n-1)$ divided by the gas density and the dimensionless ratio $\rho = \mathrm{Re}(n-1)/\mathrm{Im}(n-1)$. These results are collected in Table I for a lithium beam mean velocity $u = 1075 \pm 20$ m/s and we have similar data for several other velocities.

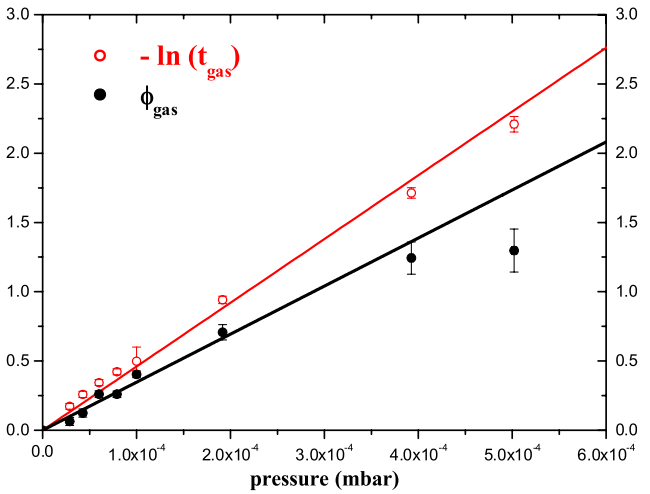

FIG. 2 (color online). Plot of the measured values of the phase shift $\varphi(n_{\mathrm{gas}})$ and of the logarithm of the amplitude transmission $-\ln[t(n_{\mathrm{gas}})]$ as a function of xenon pressure p_{cell}. The lithium beam mean velocity is $u = 1075 \pm 20$ m/s.

TABLE I. Index of refraction of argon, krypton and xenon for lithium waves with a mean velocity $u = 1075 \pm 20$ m/s. For each gas, we give the real and imaginary parts of $10^{29}(n-1)/n_{\mathrm{gas}}$ (n_{gas} in m^{-3}) and the ratio $\rho = \mathrm{Re}(n-1)/\mathrm{Im}(n-1)$.

Gas	Ar	Kr	Xe
$10^{29}\mathrm{Re}(n-1)/n_{\mathrm{gas}}$	1.20 ± 0.11	1.57 ± 0.10	1.82 ± 0.07
$10^{29}\mathrm{Im}(n-1)/n_{\mathrm{gas}}$	2.11 ± 0.06	1.99 ± 0.07	2.40 ± 0.06
ρ	0.56 ± 0.05	0.78 ± 0.04	0.70 ± 0.03

The imaginary part of the index of refraction, which measures the attenuation of the atomic beam by the gas, is related to the total collision cross section $\langle\sigma\rangle$ by $\langle\sigma\rangle = 2\mathrm{Im}(n-1)k/n_{\mathrm{gas}}$ where $\langle\,\rangle$ designates the average over the target gas thermal velocity. Figure 3 compares the cross section $\langle\sigma\rangle$ deduced from our index measurements with the values obtained by scattering techniques [18,19]: the agreement is very good, although the velocity distribution of our lithium beam, with a full width at half maximum close to 25%, is broader than the 4.4% FWHM distribution used in Refs. [18,19].

From theory [15,16], we know that $(n-1)$ decreases with the lithium velocity u, like $u^{-7/5}$, with glory oscillations superimposed on this variation. We suppress this rapid variation by plotting the real and imaginary parts of $u^{7/5}(n-1)/n_{\mathrm{gas}}$: Fig. 4 presents such a plot in the case of xenon, with our measurements and calculated values obtained by Champenois in her thesis [15] using the Buckingham-Corner potential fitted by Dehmer and Wharton [19].

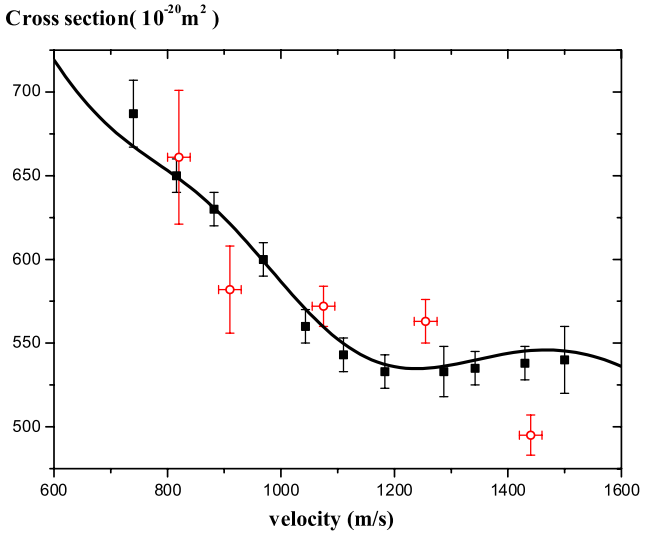

FIG. 3 (color online). Plot of the lithium-xenon total collision cross section $\langle\sigma\rangle$ as a function of the lithium mean velocity u in meters per second: our measurements by atom interferometry (open circles), measurements of Dehmer and Wharton (squares), and calculated values (full curve) obtained with the Buckingham-Corner potential fitted by these authors [19].

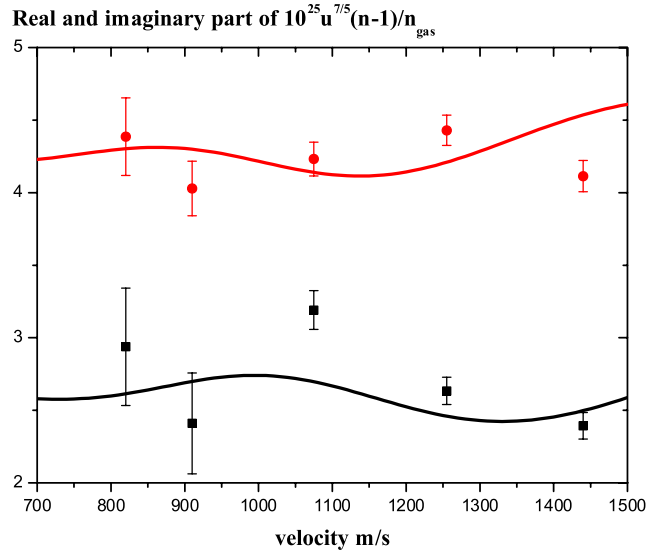

FIG. 4 (color online). Plot of the real (squares) and imaginary (dots) parts of $10^{25}u^{7/5}(n-1)/n_{\mathrm{gas}}$ measured for xenon as a function of the lithium beam mean velocity u (n_{gas} in m^{-3}, u in meters per second). The full curves represent the calculated values [15], using the Buckingham-Corner potential of Ref. [19]. The agreement between the measured and calculated values is good, especially as there are no free parameters.

Figure 5 compares our measurements of the ratio $\rho = \mathrm{Re}(n-1)/\mathrm{Im}(n-1)$ with calculations. We have chosen the case of xenon for which we have more data points. The mean ρ value is lower than the $\rho = 0.726$ value predicted in [2,3] for a purely attractive r^{-6} potential. A lower mean ρ value is expected when the $n = 8, 10$ terms of the r^{-n}

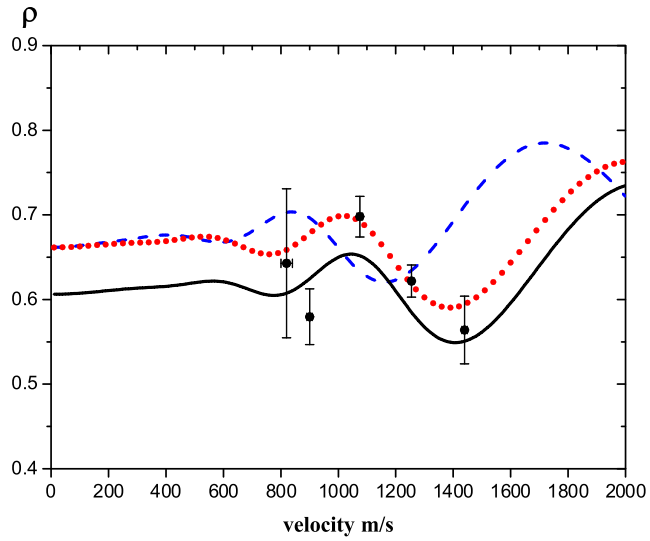

FIG. 5 (color online). Plot of the ratio $\rho = \mathrm{Re}(n-1)/\mathrm{Im}(n-1)$ for xenon as a function of the lithium beam mean velocity u. The points are our experimental values while the curves have been calculated with the lithium-xenon potential of Ref. [19] (full line), Ref. [22] (dotted line), and Ref. [23] (dashed line).

expansion of the long range potential are also attractive and not negligible [15]. Moreover, a glory oscillation is clearly visible on our measurements as well as on the calculations done by Champenois [16] with three different potential curves: two *ab initio* potentials [22,23] and the Buckingham-Corner potential of Dehmer and Wharton [19]. The three calculated curves reproduce well the observed amplitude of the glory oscillation. The observed phase is close to the calculated phase for the potentials of Refs. [19,22] and not for the one of Ref. [23]. This is not surprising as this phase is very sensitive to the potential well depth [15].

In this Letter, we have described the first measurements of the index of refraction of gases for lithium waves, with an experiment similar to those performed with sodium waves [2,3,5]. A gas cell, introduced on one of the atomic beams inside an atom interferometer, modifies the wave propagation and this modification is detected on the interference signals. We have measured the real and imaginary parts of the index of refraction n for three gases and several lithium velocities and we have verified the linear dependence of $(n-1)$ with the gas density n_{gas}. Our measurements of the imaginary part of $(n-1)$ are in very good agreement with previous measurements of the total cross section, and the real part, which can be measured only by atom interferometry, is also in good agreement with calculations of this quantity. Moreover, the comparison between experimental and theoretical values of the ratio $\rho = \mathrm{Re}(n-1)/\mathrm{Im}(n-1)$ is already able to favor certain interaction potentials.

We hope to improve our experiment, in particular, the septum which limits our ability to use higher velocities of the lithium beam. The measurement of the index of refraction in a larger velocity range and with an improved accuracy should then provide a stringent test of interaction potentials. However, it seems clear that index of refraction measurements cannot be inverted to provide very accurate interaction potentials, as long as the target gas is at room temperature, because thermal averaging washes out the low-energy resonances and most of the glory oscillations. An experiment with a target gas at a very low temperature should provide a lot more information [8,12,14]. Finally, if the target gas and the atomic beam were both ultracold, one could study the index of refraction in the quantum threshold regime and measure the atom-atom scattering length as well as low-energy resonances [10,13]. The collision experiment involving two ultracold atom clouds, which was made by Buggle *et al.* [24], proves the feasibility of dense enough gas targets for collision studies. The development of a cold atom interferometer coupled to such a gas target remains to be done.

Finally, the interaction of a matter wave with a gas induces decoherence. This effect was studied by Hornberger *et al.* with C_{70} in a Talbot Lau interferometer [25] and by Uys *et al.* with sodium in a Mach-Zehnder interferometer [26]: in both cases, a low pressure of gas is introduced everywhere inside the interferometer. This decoherence process depends on the momentum transferred to a particle of the wave by a collision with an atom of the scattering gas and on the interferometer geometry (separation between the two arms, size of the detector). This decoherence effect is thus quite different from the index of refraction for which all scattering events contribute.

We have received the support of CNRS MIPPU, ANR, and Région Midi Pyrénées. The technical staff, G. Bailly, D. Castex, M. Gianesin, P. Paquier, L. Polizzi, T. Ravel, and W. Volondat, has made these experiments possible. We thank former members of the group A. Miffre, C. Champenois, and N. Félix for their help and A. Cronin for fruitful advice.

*Email address: jacques.vigue@irsamc.ups-tlse.fr

[1] M. Lax, Rev. Mod. Phys. **23**, 287 (1951).
[2] J. Schmiedmayer *et al.*, Phys. Rev. Lett. **74**, 1043 (1995).
[3] J. Schmiedmayer *et al.*, in *Atom interferometry*, edited by P. R. Berman (Academic Press, San Diego, 1997), p. 1.
[4] T. D. Hammond *et al.*, Braz. J. Phys. **27**, 193 (1997).
[5] T. D. Roberts *et al.*, Phys. Rev. Lett. **89**, 200406 (2002).
[6] T. D. Roberts, Ph.D. thesis, Massachusetts Institute of Technology (unpublished).
[7] R. C. Forrey *et al.*, Phys. Rev. A **54**, 2180 (1996).
[8] R. C. Forrey *et al.*, Phys. Rev. A **55**, R3311 (1997).
[9] P. J. Leo, G. Peach, and I. B. Whittingham, J. Phys. B **33**, 4779 (2000).
[10] V. Kharchenko and A. Dalgarno, Phys. Rev. A **63**, 023615 (2001).
[11] R. C. Forrey, V. Kharchenko, and A. Dalgarno, J. Phys. B **35**, L261 (2002).
[12] S. Blanchard, D. Civello, and R. C. Forrey, Phys. Rev. A **67**, 013604 (2003).
[13] J. Vigué, Phys. Rev. A **52**, 3973 (1995).
[14] E. Audouard, P. Duplaà, and J. Vigué, Europhys. Lett. **32**, 397 (1995); **37**, 311(E) (1997).
[15] C. Champenois *et al.*, J. Phys. II (France) **7**, 523 (1997).
[16] C. Champenois, Ph.D. thesis, Université P. Sabatier, 1999.
[17] H. Pauly in *Atom-Molecule Collision Theory*, edited by R. B. Bernstein (Plenum Press, New York, 1979), pp. 111–199.
[18] G. B. Ury and L. Wharton, J. Chem. Phys. **56**, 5832 (1972).
[19] P. Dehmer and L. Wharton, J. Chem. Phys. **57**, 4821 (1972).
[20] A. Miffre *et al.*, Eur. Phys. J. D **33**, 99 (2005).
[21] H. C. W. Beijerinck and N. F. Verster, J. Appl. Phys. **46**, 2083 (1975).
[22] D. Cvetko *et al.*, J. Chem. Phys. **100**, 2052 (1994).
[23] S. Patil, J. Chem. Phys. **94**, 8089 (1991).
[24] Ch. Buggle *et al.*, Phys. Rev. Lett. **93**, 173202 (2004).
[25] K. Hornberger *et al.*, Phys. Rev. Lett. **90**, 160401 (2003).
[26] H. Uys, J. D. Perreault, and A. Cronin, Phys. Rev. Lett. **95**, 150403 (2005).